https://doi.org/10.3311/PPci.20626

Periodica Polytechnica Civil Engineering, 67(2), pp. 369–381, 2023

Determination of Reinforced Fly Ash Concrete Columns' Resistance Using Nonlinear Models of Materials

Viet-Hung Dang[1], Vongchith Sykhampha[2], Truong-Thang Nguyen[2*]

[1] Department of Structural Mechanics, Faculty of Building and Industrial Construction, Hanoi University of Civil Engineering (HUCE), No.55 Giai Phong Rd., Hai Ba Trung Dist., Hanoi, Vietnam
[2] Department of Concrete Structures, Faculty of Building and Industrial Construction, Hanoi University of Civil Engineering (HUCE), No.55 Giai Phong Rd., Hai Ba Trung Dist., Hanoi, Vietnam
[*] Corresponding author, e-mail: thangnt2@huce.edu.vn

Received: 08 June 2022, Accepted: 10 January 2023, Published online: 18 January 2023

Abstract

This article introduces experimental and analytical studies on the resistance under eccentric loads of reinforced fly ash concrete (RFAC) columns, in which fly ash (FA) is used to partially replace ordinary Portland cement (OPC) with a by-mass ratio of 20%. Based on experimental results of concrete specimens with mean 28-day cylinder strength of 30 MPa, modifications on simplified bi-linear and tri-linear models of stress-strain relationships of OPC concrete specified in the Russian and Vietnamese design standards are proposed. These nonlinear deformation models are incorporated into an analytical approach to establish the resistance of RFAC columns in the form of interaction surface, associated with an assessment method for safety factor based on the principle of inverse distance weighted average (IDWA). Parameters of the proposed analytical approach are determined by test results obtained from eight RFAC column specimens having 150 × 200 (mm) rectangular cross-section, 1600 mm-height, and 4Φ14 longitudinal rebars with yield strength of 362.6 MPa. In the tests, the specimens were loaded with uniaxial eccentricities ranging from 0 to 80 mm until failed. It is shown that with ε'_{b1} = 0.0022 and k_E = 0.91, the corresponding safety factors of bi-linear and tri-linear models validated for the tested specimens are conservative and nearest to unity, proving that the proposed analytical approach is capable of closely predicting the RFAC columns' resistance.

Keywords

resistance, column, reinforced concrete, fly ash, nonlinear model

1 Introduction

In building structures, piles and columns are vertical elements transferring gravity loads downward and can be primarily considered as compression members. In real situations, due to the diversified architectural and structural arrangements from unequal column grid-lines, the variations of the members' dimensions along the building height, and the geometric imperfections, both piles and columns can be subjected to either bending moment acting about one principal axis, so-called uniaxial bending, or simultaneous bending moments about two principal axes, so-called biaxial bending. There have been a significant number of published research works on the behavior and load resistance of eccentric compression reinforced concrete (RC) members. The eccentricity-dependent strengths of the tested specimens were validated with a proposed analytical approach [1–8], which then could be developed to design provisions [9–12].

In the current global trend of sustainable construction, the utilization of industrial by-product such as fly ash (FA) for concrete to reduce the production of ordinary Portland cement (OPC) has attracted researchers' attentions for a few decades. Initially, FA was mostly utilized as an additive with a limit dose for the concrete admixture to improve workability of fresh concrete [13–20]. The actual FA amount used varies widely depending on the application, mechanical and chemical properties of FA, specification limits, as well as on the geographic location and climate. It is also specified by ACI Committee 232.2R-18 [13] that FA can be introduced in concrete either as a separately-batched material or as a component of blended cement to establish fly ash concrete (FAC). In Vietnam, the current design standard for concrete structures [12] is established based on the corresponding Russian standard [11]. However, the use of reinforced fly ash concrete (RFAC)

Cite this article as: Dang, V.-H., Sykhampha V., Nguyen T.-T. "Determination of Reinforced Fly Ash Concrete Columns' Resistance Using Nonlinear Models of Materials", Periodica Polytechnica Civil Engineering, 67(2), pp. 369–381, 2023. https://doi.org/10.3311/PPci.20626

structural members and the associated calculation method has been yet specified in the aforementioned standards. As far as FA is considered an additive in concrete, it is common in practice that RFAC structures are calculated similarly to those made from OPC concrete having the same compressive strength [11, 12]. This may lead to an inaccurate prediction of the RFAC columns' eccentric loads resistance, since the presence of FA produces different stress-strain relationship of FAC although the compressive strength is kept unchanged, compared to those of OPC concrete. Among the research works published on RFAC columns [21–31], there have been limited analytical models to be proposed based on material models. This fact motivated the authors to perform experimental and analytical studies on the resistance under eccentric load of a number of eight RFAC columns with a by-mass replacement percentage of 20% for FA/OPC, which was proved to gain more favorable mechanical properties compared to the original OPC concrete having mean cylinder compressive strength of 30 MPa. The column specimens' resistance was experimentally measured with eccentricities ranging from 0, 40 and 80 mm and were compared to the results of the nonlinear deformation method proposed by the authors.

2 Research significance

In this article, the following research objectives are achieved: (i) Bi-linear and tri-linear stress-strain relationships of OPC concrete specified in some national design provisions [11, 12] are modified based on the experimental results obtained from material tests to propose nonlinear deformation models of FAC; (ii) An analytical approach incorporating the proposed material models is developed to establish the RFAC columns' resistance in the form of interaction surface, associated with an assessment method for safety factor; and (iii) The proposed analytical models are well validated by structural experiments conducted on RFAC column specimens subjected to different levels of load eccentricities. It is shown that the safety factor validated by experiments is close to and smaller than unity, meaning that the proposed approach is capable of predicting the RFAC columns' resistance under eccentric loads in a conservative manor.

3 Mechanical properties of FA concrete

An experimental program was conducted to determine the FA concrete mixture that is capable of providing more favorable mechanical properties compared to those of the control OPC concrete having mean cylinder compressive strength of 30 MPa. The original OPC concrete mixture, namely MS-30-00, consists of OPC, fine aggregate, coarse aggregate and water with the corresponding weight of 380, 760, 1140 and 205 kg, respectively. Then, the OPC mass is replaced by 20% by FA, whereas all the remaining materials are kept unchanged, establishing the corresponding mixture of MS-30-20 (Table 1).

The materials used for FA concrete mixtures in this experimental program consist of: (i) Fly ash having specific gravity of 1.80 g/cm^3, loss on ignition of 0.47, Blaine fineness (specific surface area) ranging from 1686 to 1891 cm^2/g, chemical compositions of $SiO_2 + Al_2O_3 + Fe_2O_3$ (79.25%) and CaO (5.49%). More detailed information on the granulometry, composition and mechanical properties of the FA used in this research can be referred to in [33]; (ii) Local ordinary Portland cement (OPC) with specific gravity of 3.10 g/cm^3; (iii) Fine aggregate with unit weight of 2.64 g/cm^3; (iv) Coarse aggregate with unit weight of 2.69 g/cm^3; and (v) Domestic water.

It should be noted in Table 1 that: (i) The total binder weight and water/binder ratio were both kept constant at 380 kg and 0.54 for all the mixtures, respectively; and (ii) Due to the difference between OPC and FA specific gravities, there is an increment in total FA concrete volume when OPC is replaced by FA. Then, the proportions calculated for 1 m^3 FA concrete are put in parentheses in Table 1.

A significant number of 150 × 300 mm-cylinder and 150 mm-cube concrete samples were prepared for testing at 7, 14, 28, 56 and 90-day ages, with three samples for every testing group. The tests were prepared and conducted at Laboratory LAS-XD 125, Hanoi University of Civil Engineering (HUCE), Vietnam, conforming the related international testing standards [32].

The cylinder compressive strength at the ages of 7, 14, 28, 56 and 90 days as well as the split tensile strength measured for MS-30-00 and MS-30-20 are shown Table 2. The standard deviation values are shown in parentheses.

Table 1 Mixtures of concrete

Mixtures	FA/OPC replacement percentage	Binder (kg)		Fine aggregate (kg)	Coarse aggregate (kg)	Water (l)
		OPC	Fly ash			
MS-30-00	0%	380	0	760	1140	205
MS-30-20	20%	304 (298.7)	76 (74.7)	760 (746.8)	1140 (1120.2)	205 (201.4)

Table 2 Experimental results of concrete strength

Concrete mixture	Compressive strength (MPa) at the ages of					28-day tensile split strength (MPa)
	7 days	14 days	28 days	56 days	90 days	
MS-30-00	16.07 (0.06)	20.84 (0.035)	30.44 (0.115)	30.61 (0.205)	31.31 (0.329)	2.78 (0.201)
MS-30-20	13.51 (0.146)	20.35 (0.428)	31.10 (0.172)	32.03 (1.114)	32.48 (1.161)	3.07 (0.312)

It can be seen that from the age of 28 days, MS-30-20 performed better than MS-30-00 in terms of both cylinder compressive strength and split tensile strength.

The stress-strain relationships of unconfined cylinder concrete specimens for MS-30-00 and MS-30-20 admixtures are shown in Fig. 1 [33].

It can be seen from the experimental results that the 20% FA concrete mixture MS-30-20 has more favorable mechanical properties in terms of compressive strength and its' development, split tensile strength compared to MS-30-00. The different in stress-strain relationship between the two mixtures will be used in the analytical analysis.

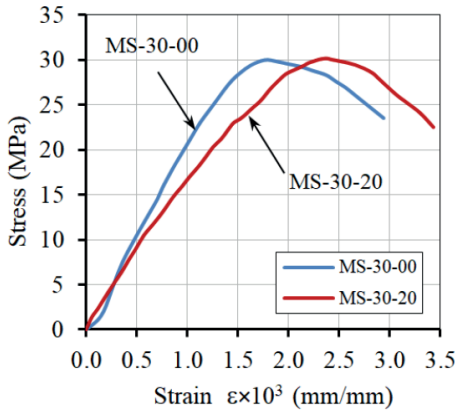

Fig. 1 Test results on stress-strain relationship of FAC

4 Analytical approach

4.1 Nonlinear deformation models for FA concrete

In this proposed analytical approach, the FA concrete's nonlinear deformation models are established by simplifying the experimental stress-strain relationship shown in Fig. 1 associated with a modification of the corresponding nonlinear model for OPC concrete specified in [11, 12], which are in the forms of bi-linear and tri-linear models as shown in Figs. 2(a) and 2(b), respectively.

In the bi-linear deformation model of OPC concrete, the compressive stress σ_b can be determined from the strain and elastic modulus as follows [11, 12]:

$$\sigma_b = E_{b,red}\varepsilon_b \text{ when } 0 \le \varepsilon_b < \varepsilon_{b1}, \quad (1)$$

$$\sigma_b = R_b \text{ when } \varepsilon_{b1} \le \varepsilon_b < \varepsilon_{b2}, \quad (2)$$

where $\varepsilon_{b1} = \varepsilon_{b1,red} = 0.0015$; $\varepsilon_{b,red} = R_b/\varepsilon_{b1,red}$; $\varepsilon_{b1} = 0.0035$ and R_b is the design cube compressive strength of OPC concrete.

In the modification of bi-linear deformation for FA concrete, based on Fig. 2(a) and Table 1, it is proposed by the authors that $\varepsilon_{b2} = \varepsilon'_{b2} = 0.0035$ and ε'_{b1} will be varied from 0.0015 to 0.0025 to determine the most appropriate value based on test results.

The tri-linear deformation model of OPC concrete can be expressed as [11, 12]:

$$\sigma_b = \varepsilon_b E_b \text{ when } 0 \le \varepsilon_b < \varepsilon_{b1}, \quad (3)$$

$$\sigma_b = \left[\left(1 - \frac{\sigma_{b1}}{R_b}\right)\frac{\varepsilon_b - \varepsilon_{b1}}{\varepsilon_{b0} - \varepsilon_{b1}} + \frac{\sigma_{b1}}{R_b}\right]R_b \text{ when } \varepsilon_{b1} \le \varepsilon_b < \varepsilon_{b0} \quad (4)$$

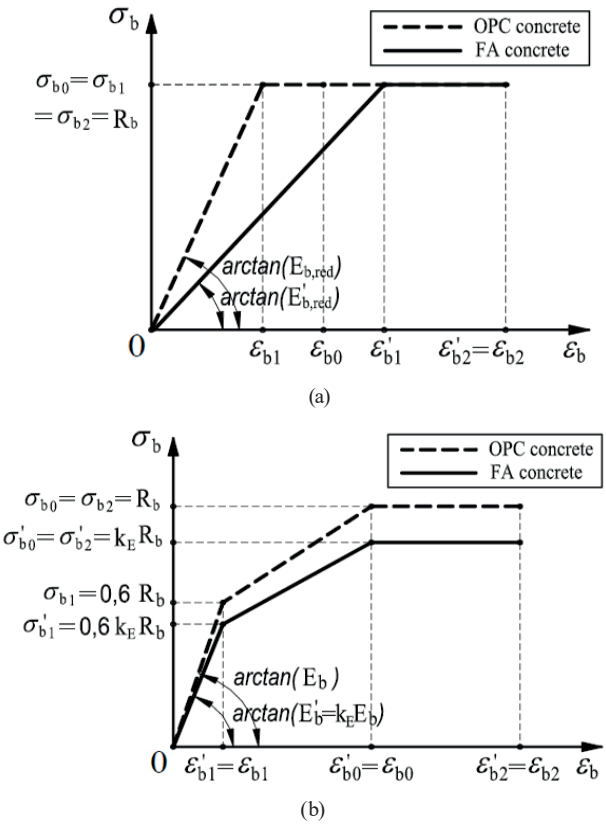

Fig. 2 a) Bi-linear model (B-LM); b) Tri-linear model (T-LM)

$$\sigma_b = R_b \text{ when } \varepsilon_{b0} \le \varepsilon_b < \varepsilon_{b2} \quad (5)$$

where $\varepsilon_{b0} = 0.002$; $\sigma_{b1} = 0.6R_b$; $\varepsilon_{b1} = 0.6R_b/E_b$; ε_{b2} is similar to that of the bi-linear model; E_b is the elastic modulus of OPC concrete.

In the modification of the tri-linear deformation model for FA concrete, based on Fig. 2(b), one gets $R'_b = k_E R'_b$ where the factor k_E is to account for the reduction in elastic modulus of FA concrete (E'_b) compared to that of OPC concrete (E_b). In this analytical approach, it is proposed that all the strain limits are kept constant, such as $\sigma'_{b1} = \sigma_{b1}$; $\varepsilon'_{b0} = \varepsilon_{b0} = 0.002$ and $\varepsilon_{b2} = \varepsilon'_{b2} = 0.0035$ (Fig. 2(b)), whereas the reduction factor k_E will be varied from 0.85 to 0.95 to determine the most appropriate value based on test results.

In the analytical approach proposed this article, the bi-linear material model for reinforcing steel specified in [11, 12] shown in Fig. 3 is also utilized.

In the bi-linear model for reinforcing steel (Fig. 3), stress can be calculated from strain and elastic modulus with $\varepsilon_{s0} = R_s/E_s$ and $\varepsilon_{s2} = 0.0025$ as follows:

$$\sigma_s = E_s \varepsilon_s \ when \ 0 \le \varepsilon_s < \varepsilon_{s0}, \tag{6}$$

$$\sigma_s = R_s \ when \ \varepsilon_{s0} \le \varepsilon_s < \varepsilon_{s2}, \tag{7}$$

where $\sigma_{s1} = 0.9R_s$; $\varepsilon_{s1} = 0.9R_s/E_s$; $\varepsilon_{s2} = 0.015$; $\varepsilon_{s0} = R_s/E_s$ and $\varepsilon_{s0} = R_s/E_s + 0.0002$ for reinforcing steel having actual and conventional yield strength, respectively.

4.2 Principles of cross-sectional analysis for columns

The following conventional assumptions are incorporated into the analysis: (i) The distribution of strains in concrete and steel reinforcement along the cross-section height is linear (plane strain assumption); (ii) Nonlinear deformation models introduced in Section 4.1 are used for concrete; and (iii) Concrete tensile stress is ignorable.

The resistance on normal section of both RC and RFAC columns can be determined from the condition for ultimate strains: $|\varepsilon_{b,\max}| \le \varepsilon_{bu}$; $\varepsilon_{s,\max} \le \varepsilon_{bu}$. The ultimate strains values of materials can be calculated as follows: (i) When neutral axis is within the column's cross section:

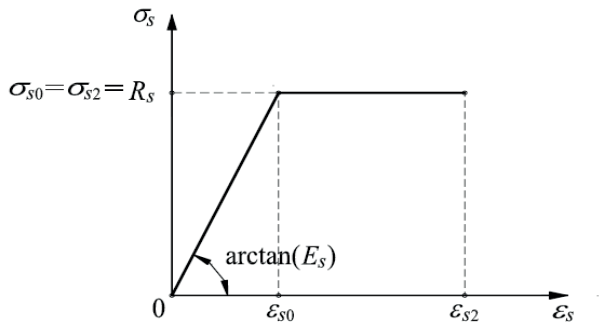

Fig. 3 Bi-linear deformation model for reinforcing steel

$\varepsilon_{b,u} = \varepsilon_{b2} = 0.0035$; (ii) When neutral axis is out of the cross section: $\varepsilon_{b,u} = \varepsilon_{b2} - (\varepsilon_{b2} - \varepsilon_{b0})\varepsilon_1/\varepsilon_2$ where $\varepsilon_{b0} = 0.002$; ε_1 and ε_2 are the strains at opposite extreme fibers and $|\varepsilon_2| \ge \varepsilon_1$; and (iii) For reinforcing steel, $\varepsilon_{s,u} = 0.0025$.

Consider a rectangular column subjected to an axial load N with eccentricities e_y and e_x corresponding to bending moments $M_y = Ne_x$ and $M_x = Ne_y$ (Fig. 4).

An arbitrary neutral axis (n.a) can be expressed by its angle β with X-axis and the distance C_n to point A. Each neutral axis is corresponding to a set of ultimate forces resistance (N_u, M_{xu}, M_{yu}), which can be determined by setting the concrete strain of extreme fiber at point A equal to $\varepsilon_{b,u}$. Gradually increase angle β from 0 to 90° and put C_n into an iteration loop, the column load resistance can be established in the form of interaction surface following the below equilibrium conditions:

$$M_x = \sum_{i=1}^{n}\sum_{j=1}^{m} \sigma_{bij} A_{bij} Z_{bxi} + \sum_{k=1}^{p} \sigma_{sk} A_{sk} Z_{sxk}, \tag{8}$$

$$M_y = \sum_{i=1}^{n}\sum_{j=1}^{m} \sigma_{bij} A_{bij} Z_{byij} + \sum_{k=1}^{p} \sigma_{sk} A_{sk} Z_{syk}, \tag{9}$$

$$N = \sum_{i=1}^{n}\sum_{j=1}^{m} \sigma_{bij} A_{bij} + \sum_{k=1}^{p} \sigma_{sk} A_{sk}, \tag{10}$$

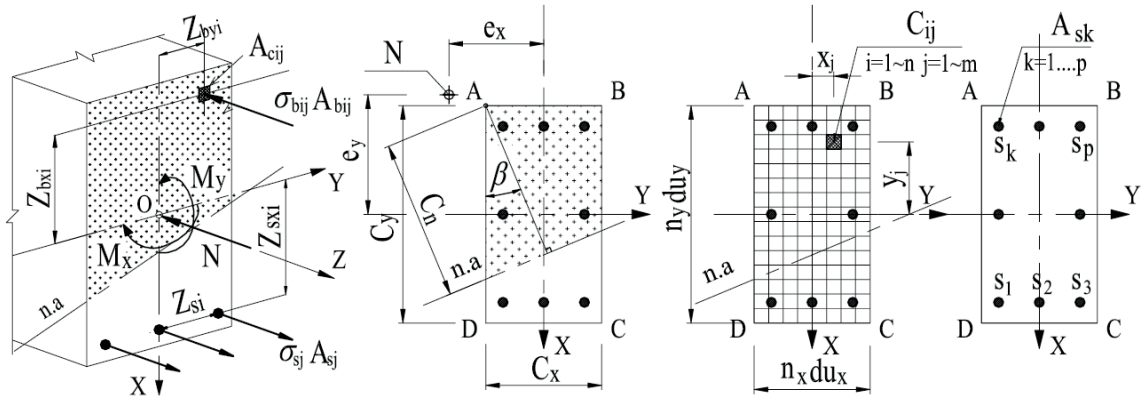

Fig. 4 Discretization of column cross section a) 3D view; b) Position of neutral axis; c) Modeling of concrete; d) Modeling of rebars

where m and n are the sizes of the two-dimensional array of ($m \times n$) rectangular concrete sub-elements having a unique area of $A_{cij} = du_x \times du_y (i = 1 \sim m, j = 1 \sim n)$ and a number of round-shaped sub-elements representing reinforcing bars (rebars), namely, S_1 to S_p, with the corresponding areas $A_{sk} = (k = 1 \sim p)$ (Figs. 4(b, c)). The compressive stress σ_{cij} is assumed to be uniformly distributed within a sub-element.

The resistance of the column (N_u, M_{xu}, M_{yu}) can be expressed in the form of an interaction surface as shown in Fig. 5. It is noteworthy that when angle β equals to 0 and 90°, one obtains the cases of uniaxial bending resistances (N_u, M_{xu}) and (N_u, M_{yu}) of the cross-section principal planes parallel with X- and Y-axis, respectively.

4.3 Moment magnification factor

In [11, 12], the moment magnification factor (MMF) is specified as $\eta = 1/(1 - N/N_{cr})$ where N is the acting axial force; N_{cr} is the conventional Euler load $N_{cr} = \pi^2 D/L_0^2$; D is the stiffness od reinforced concrete section $D = k_b E_b I_b + k_s E_s I_s$; E_b and E_s are elastic moduli of concrete and reinforcing steel, respectively; I_b and I_s are the moments of inertia of the concrete and rebars areas to cross-section's centroidal axes, $I_{bx} = C_v C_x^3/12$ and $I_{sx} = \sum A_{sk} y_{sk}^2$; $I_{by} = C_x C_y^3/12$ and $I_{sy} = \sum A_{sk} x_{sk}^2$, respectively. The parameter k_s taking into account the reinforcing steel stiffness is set to 0.7; $k_b = 0.15/[\varphi_L(0.3 + \delta_e)]$; $\varphi_l = 1 + M_L/M_{L1} \leq 2$; M_L and M_{L1} are respective bending moments to the centroid of the extreme tensile rebars of the whole loads and of the long-term loads acting on the cross-section. To validate with experiments which was conducted under short-term loading condition, one can give $\varphi_l = 1$; $\delta_e = e_0/h$ and is within the range from 0,15 to 1,50; e_0 is the initial eccentricity; $e_0 = \max(M/N, e_a)$ for indeterminate structures and $e_0 = M/N + e_a$ for determinate structures; e_a is the accidental eccentricity, in a principal bending plane of column's cross-section parallel to cross-section side h, $e_a = \max(L/600, h/30, 10\text{ mm})$, where L is the column height.

For each critical set of acting loads (N, M_x, M_y), there will be a corresponding couple of moment magnification factors for two principal bending planes of the cross-section (η_x, η_y). Then, the set of design load (N, η_x, M_x, η_y, M_y) can be determined and evaluated with the column strength in the form of interaction surface (N_u, M_{xu}, M_{yu}) determined in Section 4.2.

4.4 Assessment of safety factor

For the experimental validation purpose, the safety factor can be determined based on the in-space relative position of a point L representing the test failure load by coordinates (N, η_x, M_x, η_y, M_y). There exists a so-called interpolated point C (N_u, M_{xu}, M_{yu}) on the interaction surface that sits on the line connecting the origin O (0,0,0) to point L. When point L is outside the interaction surface with a ratio $CR = \overline{OL} / \overline{OC} > 1$, it is safe since the predicted column load resistance is lower than the actual failure load. Then, the proposed model is conservative when the safety factor is $FS = \overline{OC} / \overline{OL} < 1$ (Fig. 6).

In fact, the interaction surface established in Section 4.2 is only a set of individual points. Hence, an interpolation method is proposed to determine the position of point C. Based on the method of Inverse Distance Weighted Average (IDWA), the authors calculate the effect of the investigated point to the adjacent known points. In order to interpolate, the Descartes coordinate system (N, M_x, M_y) should be converted into spherical coordinate system (u, v, R) following the below expressions:

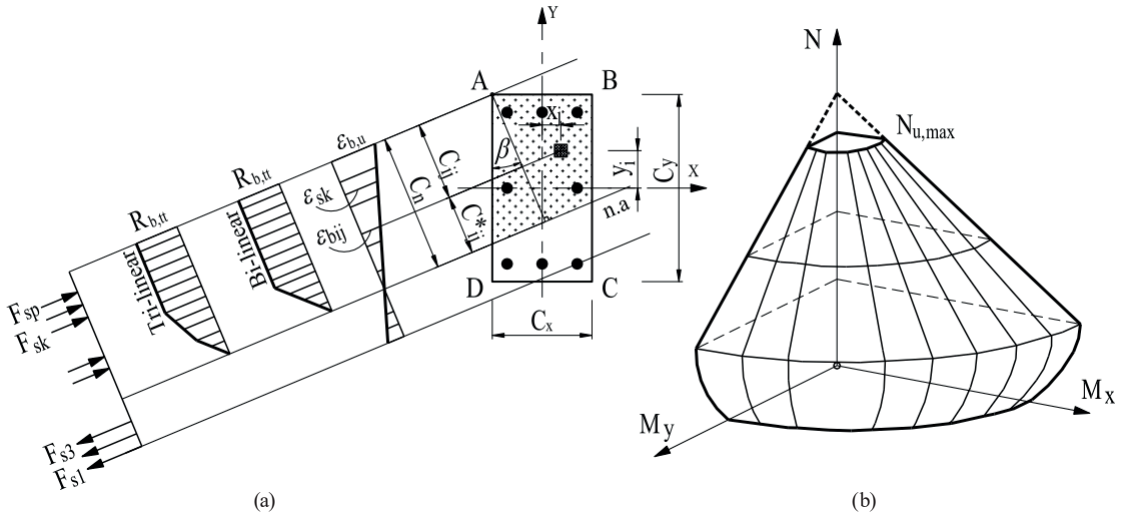

(a) (b)

Fig. 5 a) Cross-sectional analysis with an arbitrary neutral axis; b) Resistance of RFAC columns in the form of interaction surface

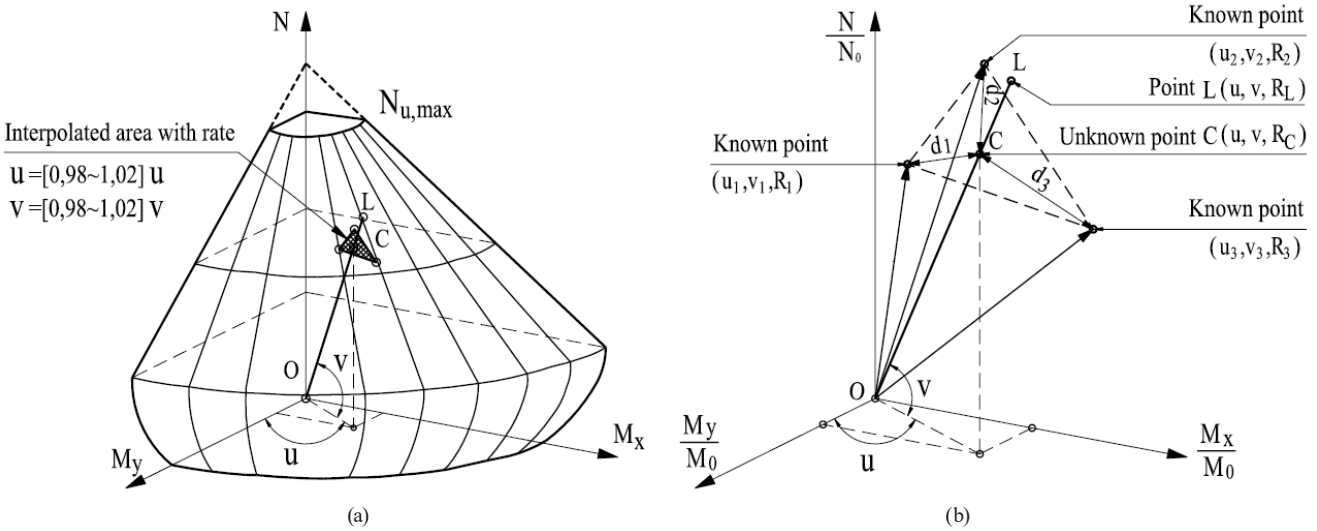

Fig. 6 a) Determination of safety factor; b) Interpolation of unknown point C from adjacent known points

$$R = \sqrt{\left(\frac{N_z}{N_0}\right)^2 + \left(\frac{M_x}{M_0}\right)^2 + \left(\frac{M_y}{M_0}\right)^2}, \tag{11}$$

$$u = \arctan\left(\frac{M_x}{M_y}\right), \tag{12}$$

$$v = \arcsin\left(\frac{N_z / N_0}{R}\right), \tag{13}$$

where N_0 and M_0 are the respective unit values of axial force and bending moment for the normalization of the term R.

In spherical coordinate system, since the interpolated point C sits on line OL, the coordinates (u, v) of point C are also the coordinates (u, v) of point L. The distance R_C from point C to point O can be calculated as below, where d_i is the distance from point C to the adjacent point number (i):

$$R_c = \frac{\sum_{i=1}^{n} R_i \frac{1}{d_i}}{\sum_{i=1}^{n} \frac{1}{d_i}}; d_i = \sqrt{(\Delta u)^2 + (\Delta v)^2}. \tag{14}$$

The above interpolation method is incorporated into the analytical approach as follows: With a set of arbitrary acting forces (N_i, M_{xi}, M_{yi}), there exists a set of parameters (u_i, v_i, R_i) calculated from Eqs. (11)–(13), where (N_i, M_{xi}, M_{yi}) are all the positive values. Based on the values of u_i and v_i, the nearest adjacent points among 5096 points of the interaction surface will be determined with a tolerance of ±2.0%. Applying Eq. (14) for the investigated points to obtain R_{ci}, the safety factor then can be determined as $FS = \overline{\mathrm{OC}} / \overline{\mathrm{OL}} = R_c / R_L$.

5 Experimental validation

5.1 Experimental program

In order to verify the analytical approach proposed in Section 4, a number of eight RFAC column specimens were cast using MS-30-20 proportion, which was initiated from OPC concrete having mean cylinder strength of 30 MPa. Basically, all the columns had identical design but were subjected to different uniaxial eccentricities of 0, 40 and 80 mm in the tests. Hence, they were divided into three corresponding groups, namely, C-30-00, C-30-40 and C-30-80, which consisted of 2, 3 and 3 specimens, respectively. Then, specimens were labeled by combining the group name with its order number in the group, i.e., C-30-00-1, C-30-00-2, C-30-40-1, C-30-40-2, C-30-40-3, C-30-80-1, C-30-80-2, and C-30-80-3.

The columns were cast in two batches. The first batch consisted of five specimens of C-30-00 and C-30-40 groups. After formwork removal, the three remaining specimens of C-30-80 group were cast in the second batch. A sufficient number of cylinder and cube concrete samples were cast together with the columns to determine the scatter of the mechanical properties of the batches.

Details and instrumentations of column specimens are shown in Fig. 7. All the test specimens had identical geometric properties of 150 × 200 mm rectangular cross-section and 1.6 m-height. Two ends of the specimen were designed with larger dimensions of 150 × 400 (in mm) to accommodate the uniaxial eccentricities that parallel to the side h of the column cross-section. Reinforcing bars and steel plates were also designed in these column heads to avoid local failure in the tests.

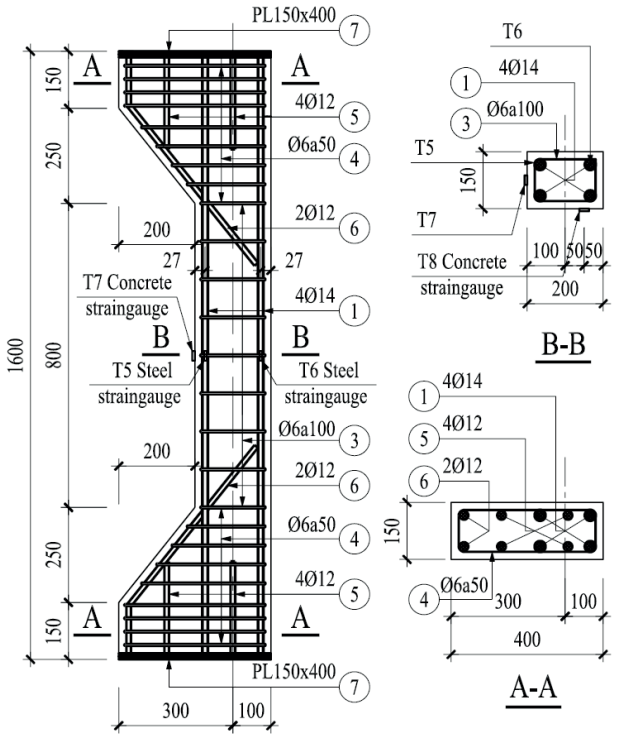

Fig. 7 Details of RFAC column specimens

All column specimens were reinforced with four 14 mm-diameter longitudinal reinforcing bars (4Φ14), which had mean yield strength of f_y = 362.6 MPa, and 6 mm-diameter stirrups at a distance of 100 mm (ϕ6@100). C-30-00 and C-30-40 specimens, which were both cast in the first batch, had design concrete cylinder strength of f_{cd} = 24.613 MPa. For C-30-80 specimens, the concrete cylinder strength was f_{cd} = 24.386 MPa.

It can be seen in Fig. 7 that a number of steel strain gauges were bonded to longitudinal rebars at the column mid-height cross section. Concrete strain gauges were also mounted at the compression surface at the column's mid-height. The steel and concrete strain gauges were KFG-5-120-C1-11L8M3R and TML PL-60-11-5LT with gauge factors of 2.07 and 2.12 (±1%), respectively. Fig. 8 illustrates the test set-up for determining the resistance of RFAC columns subjected to different levels of eccentricity. The test specimen was installed inside the frame of a hydraulic compression machine and was subjected to an axial load from the upper end. The lower end of the specimen was connected to the base having a Φ30 mm steel rod so that the column could be tested in pinned and pinned-on-roller end conditions. The eccentricity was produced by the distance between the column centroidal axis and the rollers. A load cell was positioned in between the machine and the specimen. Longitudinal deformation of the column was measured by four linear variable displacement transducers (LVDTs), namely, T1, T2, T3 and T4, that were installed around the four sides of the cross-section at the mid-height of the specimen. Lateral deformation at column's mid-height was measured by LVDT I2. Another two LVDTs, I1 and I3 were located at 150 mm from the column ends for checking purpose. Strains in concrete and longitudinal rebars were measured from the corresponding steel and concrete gauges instrumented before the tests. This test setup was chosen owing to these reasons: (i) The load eccentricity is produced at both ends of the specimens, where there are pined connections; and (ii) Material failure is to be occurred at the mid-height cross section of the specimen when its load resistance is reached.

After being installed into the test frame and instrumented by LVDTs, RFAC column specimens were tested following this procedure: (1) Preload to 5% of the predicted axial resistance of the column that was according to local design equations [12] and then unload to eliminate all slacks that possibly existed in the system; (2) Initialize

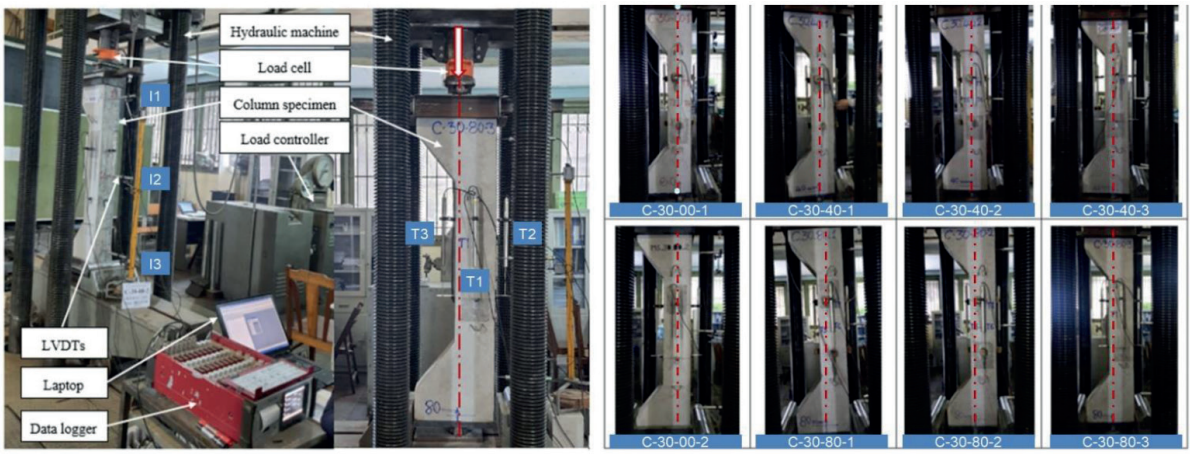

Fig. 8 Test set-up and test specimens

all instrumentation; and (3) Load in a load-controlled mode at a constant rate of 10 kN/min until the applied load could not be sustained by the specimen. The maximum load recorded was the experimental axial resistance of the test column. All the remaining data were recorded by the data-logger at 2-second intervals (Fig. 8).

5.2 Experimental results

Experimental relationship between the axial load N_{test} measured by the load-cell and lateral deflection Δ_{test} at the column mid-height measured by LVDT I2 of all the specimens are shown in Fig. 9

It can be observed in Fig. 9 that:

- The N_{test}–Δ_{test} curves of the column specimens in a series are relatively close to each other, showing the reliability of the test program;
- The N_{test}–Δ_{test} curves of C-30-80 series have lowest slope value whereas those of C-30-00 and C-30-40 series have the highest and the medium values, respectively. That means that when the initial eccentricity increases, the increment rate of the lateral displacement at the column mid-height section also increases.

The initial eccentricity is determined as $e_0 = e_1 + e_a$, where e_1 is the static eccentricity and equals to 0, 40 and 80 mm corresponding to the three groups; e_a is the accidental eccentricity that can be determined as e_a = max(L_c/600; h_c/30,10 mm) = 10 mm. Hence, the initial eccentricities of the groups C-30-00, C-30-40 and C-30-80 were 10, 50 and 90 mm, respectively. The maximum bending moment at column mid-height corresponding to the maximum axial load then can be calculated as $M_{test} = N_{test}e_0 + \Delta_{test}$. The calculated values are shown in Table 3. It should be noted that the ratio $(e_0 + \Delta_{test})/ e_0$ is also the experimental bending moment magnification ratio.

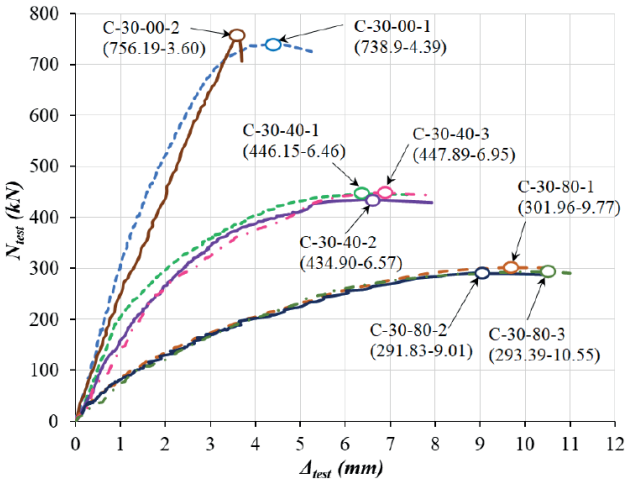

Fig. 9 Experimental results of N_{test}–Δ_{test} curves

The test results of strain in the mid-height cross-section of C-30-80-1 are shown in Fig. 10 as a typical example. The similar results were also obtained for the remaining column groups of C-30-00 and C-30-40.

Fig. 10 shows the values measured from concrete strain-gauges T7 and T8 (which were at the respective distances of 200 and 150 mm from the extreme tensile fibers) and steel strain-gauges T5 and T6 (which were at the respective distances of 173 and 27 mm from the extreme tensile fibers) (Fig. 10(b)). It can be seen from Fig. 10(a) that T5, T7 and T8 constantly developed in compression while T6 was always in tension. When the corresponding measured values of T7, T5, T8, T6 at the load levels of 20, 40, 60, 80 and 95% of the failure load were put in the same figure, it is clearly shown in Fig. 10(b) that the plane strain assumption was validated at the load levels of 20, 40, 60 and 80%, and could be relatively accepted in the load level of 95%.

Images of the typical failed specimens in each testing group are shown in Fig. 11. It is shown that the failure occurred at the column's mid-height section, where concrete at compression zone crushes and cracks developed severely in the tension zone, indicating material failure at ultimate limit state. Hence, the cross-sectional analysis based on the analytical approach introduced in Section 4 shall be applied for verification purpose.

5.3 Validation for RFAC columns

The experimental load resistance of the eight RFAC column specimens tested in Sections 5.1 and 5.2 can be used to determined the un-known parameters ε'_{b1} and k_E that are respectively proposed in bi-linear and tri-linear models for FA concrete as presented in Section 3.1 and

Table 3 Experimental results on load resistance of RFAC columns

Group	C-30-00 (e_1 = 0)		C-30-40 (e_1 = 40 mm)			C-30-80 (e_1 = 80 mm)		
Specimen	No.1	No.2	No.1	No.2	No.3	No.1	No.2	No.3
N_{test} (kN)	738.90	756.19	446.15	434.90	447.89	301.96	291.83	293.39
Δ_{test} (mm)	4.39	3.60	6.46	6.57	6.95	9.77	9.01	10.55
M_{test} (kNm)	10.635	10.288	25.191	24.601	25.505	30.127	28.850	29.500

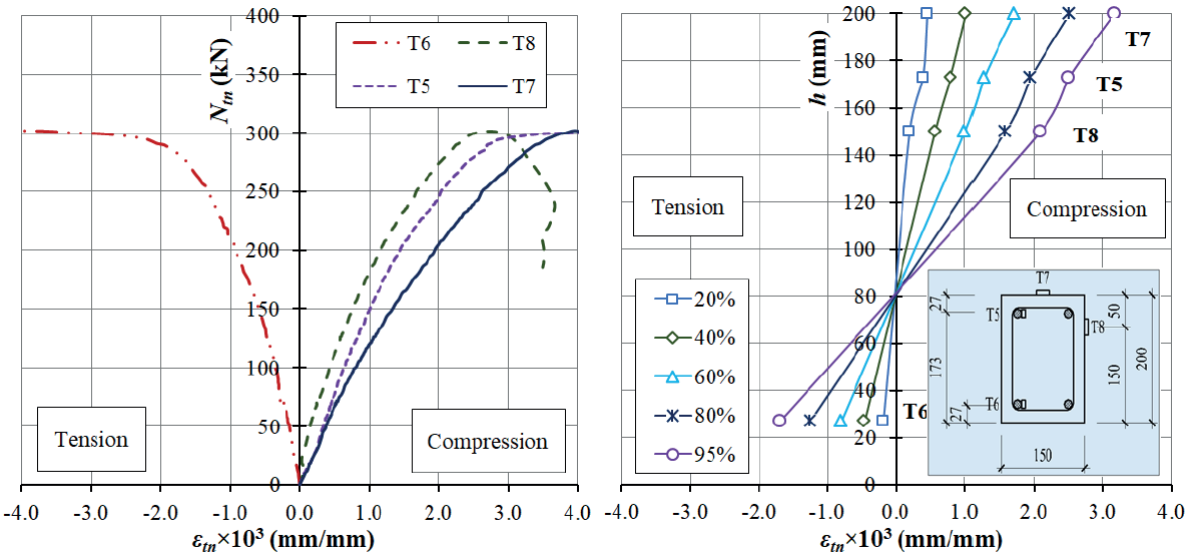

(a) (b)

Fig. 10 Measured strain at mid-height cross section of C-30-80-1 a) Strain development; b) Validation of plane strain assumption

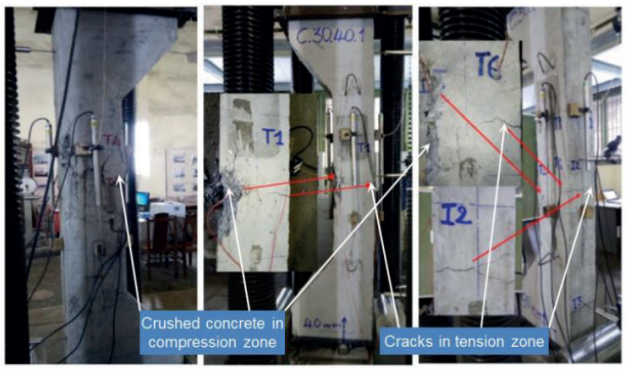

Fig. 11 Failure mode of a) C-30-00-1; b) C-30-40-1; c) C-30-80-1

shown in Figs. 3(a) and 3(b). Using trial-and-error principle to replace the values of 0.0020, 0.0021, 0.0022, 0.0023, 0.0024 and 0.0025 for ε'_{b1} (bi-linear model) and 0.85, 0.87, 0.89, 0.91, 0.93 and 0.95 for k_E (tri-linear model) into the analytical approach proposed in Section 4.4 and compare to the experimental results presented in Section 5.2. The appropriate values of and can be determined when the corresponding safety factor obtained from Section 4.4 is smaller than and nearest to unity. The results for RFAC columns in C-30-00, C-30-40 and C-30-80 series with ε'_{b1} = 0.0025 and k_E = 0.85 are respectively shown in Figs. 12, 13 and 14 for illustration.

The safety factors calculated in the proposed analytical approach for FA concrete (for both bi-linear model - B-LM, and tri-linear model - T-LM) are listed in Table 4.

It can be observed from Figs. 12, 13, 14 and Table 4 for the comparison results that:

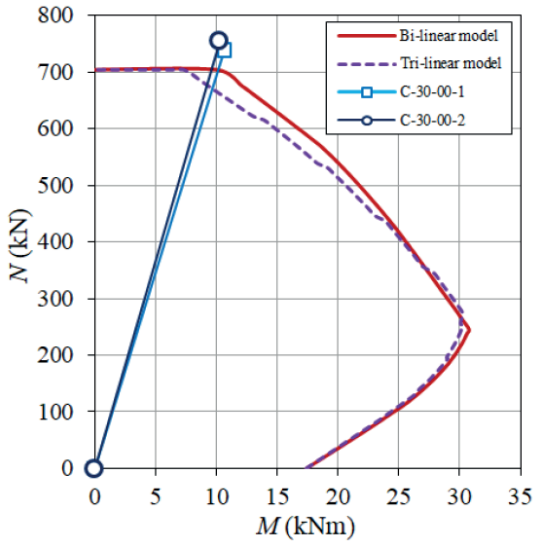

Fig. 12 Validation for C-30-00 group

- When the nonlinear models for FA concrete proposed in Fig. 2 are incorporated, it can be seen that that all the failure load (point L) of eight tested RFAC columns are all outside of the interaction diagram, with all the safety factors shown in Table 4 smaller than and close to unity (ranging from 0.902 to 0.996). This means the proposed material nonlinear models are capable of predicting closely and conservatively the eccentric load resistance of RFAC columns;
- It is shown from Table 4 that the validation results in each group are all in good agreement since the coefficient of variation (COV) is insignificant (ranging from 0.008 to 0.023);

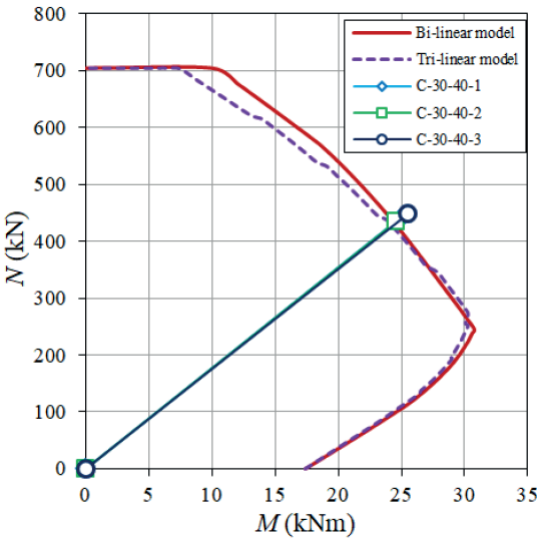

Fig. 13 Validation for C-30-40 group

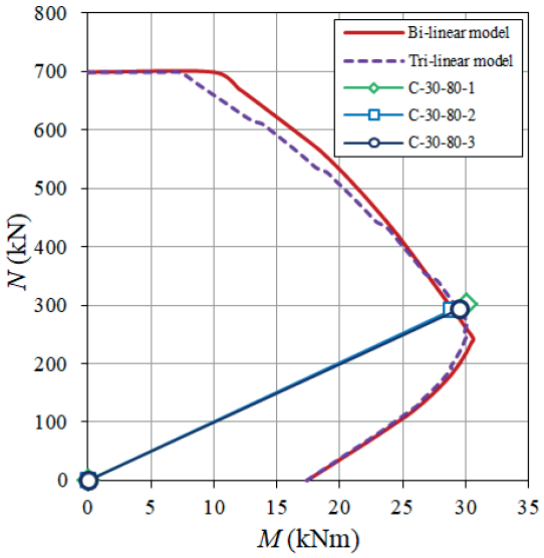

Fig. 14 Validation for C-30-80 group

Table 4 Safety factor determined on the tested RFAC columns with $\varepsilon'_{b1} = 0.0025$ and $k_E = 0.85$

Group	C-30-00 ($e_1 = 0$)		C-30-40 ($e_1 = 40$ mm)			C-30-80 ($e_1 = 80$ mm)		
Specimen	No.1	No.2	No.1	No.2	No.3	No.1	No.2	No.3
SF for B-LM	0.942	0.927	0.970	0.994	0.961	0.963	1.004	0.986
Mean (COV)	0.935 (0.011)			0.975 (0.017)			0.984 (0.021)	
Grand mean value				0.955				
SF for T-LM	0.908	0.896	0.961	0.984	0.952	0.975	1.016	0.998
Mean (COV)	0.902 (0.008)			0.966 (0.017)			0.996 (0.021)	
Grand mean value				0.965				

- Figs. 12, 13, 14 also show that the tri-linear model for FA concrete generally provide more conservative load resistance of RFAC columns compared to that of bi-linear model, since the T-LM curves are always under the B-LM's.

It can also be seen in Table 4 that with $\varepsilon'_{b1} = 0.0025$ and $k_E = 0.85$, the grand average values of safety factor *SF* for bi-linear and tri-linear models are 0.955 (calculated from individual group *SF* of 0.935, 0.975 and 0.984) and 0.965 (from 0.902, 0.966 and 0.996), respectively. Similar procedure for the remaining values of ε'_{b1} and k_E is applied to determine the corresponding grand average values of safety factor *SF*. It can be seen from Figs. 15 and 16 that:

- For the proposed bi-linear model, the safety factor *SF* decreases with an increment of ε'_{b1}. At $\varepsilon'_{b1} = 0.0021$, one gets $SF > 1$. When $\varepsilon'_{b1} = 0.0022$, $SF = 0.994$ (see Fig. 15);
- For the proposed tri-linear model (Fig. 16), *SF* and k_E are proportional. When $k_E = 0.91$, it produces the safety factor value of $SF = 0.997$.

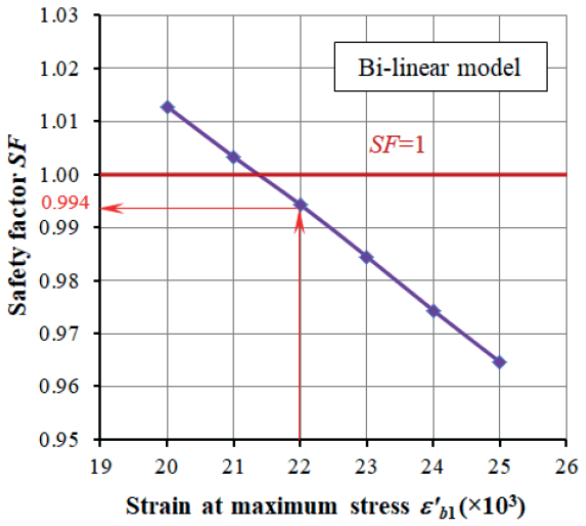

Fig. 15 Determination of analytical value of ε'_{b1}

It can be explained from Fig. 2 and Fig. 5 that when ε'_{b1} increases or k_E decreases, the column resistance will decrease, leading to a regression of the interaction diagram in Figs. 12–14. As a result, the safety factor *SF* shown in Fig. 6 will decrease.

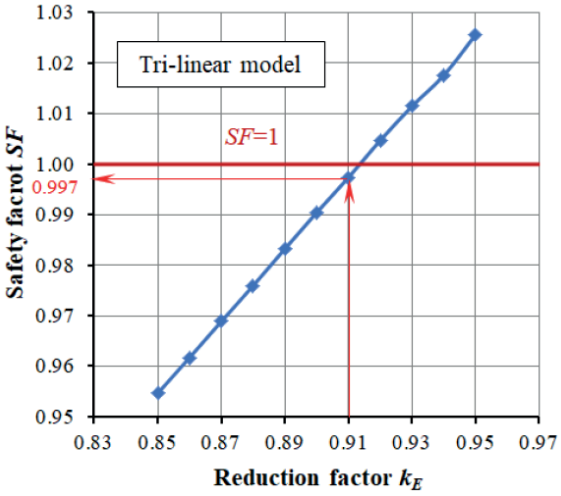

Fig. 16 Determination of analytical value of k_E

Hence, the analytical values of the proposed bi-linear and tri-linear models for FA concrete to determine the resistance of RFAC columns under eccentric loads are the values smaller than and nearest to unity compared to the remaining investigated cases. They are ε'_{b1} = 0.0022 and k_E = 0.91, respectively.

6 Discussions

In this article, experimental and analytical approaches are performed to determine the load resistance of RFAC columns subjected to axial loads with various values of eccentricity. Experimental studies are conducted in both material and structural levels. The material tests on concrete samples provide the premise for the analytical approach proposed whereas the structural tests on RFAC column specimens are for the validation purpose.

Based on the material tests, it is shown in the stress-strain relationship in Fig. 1 that although the compressive strength is not reduced, there is a certain increment in the ultimate strain as well as a reduction in elastic modulus of FAC, compared to those of the original OPC concrete before 20% of cement mass is replaced by FA. This is a basis to propose the nonlinear deformation models of FAC in the forms of simplified bi-linear and tri-linear stress-strain relationships shown in Fig. 2. The models are proposed with pre-assumed ranges of the ultimate strain ε'_{b1} (for bi-linear model) and the reduction factor k_E (for tri-linear model), which both account for the disadvantage effect of FA to the mechanical properties of FAC.

In the analytical approach proposed in this study, a number of new calculation techniques are adopted in the conventional sectional analysis for RFAC columns, they are: (i) An arbitrary position of neutral axis represented by a set of parameters (c_n, β) shown in Fig. 4(b) can be considered; (ii) The proposed nonlinear material models for FAC are incorporated as shown in Fig. 5(a) to establish the column biaxial bending resistance in the form of interaction surface (Fig. 5(b)); and (iii) The Inverse Distance Weighted Average (IDWA) method is utilized to determine the safety factor used in the validation (Fig. 6).

The structural tests on three groups of eight RFAC column specimens has provided the following meaningful observations: (i) The testing program is capable of capturing the load resistances of RFAC columns which are the peaks of the N-D curves shown in Fig. 9; (ii) The assumptions used in the analysis are proved to be reliable via the strain measurements shown in Fig. 10; (iii) The material failure criteria observed in Fig. 11 is proved to be the basis of the analysis; (iv) The proposed analytical is capable of predicting RFAC columns' resistance accurately and conservatively; and (v) It can also be observed from Figs. 12 to 14 that the tri-linear model provides more conservative resistance of RFAC columns since the curves in hidden lines are lower than those of bi-linear model, which are the curves in continuous lines.

7 Conclusions

A number of conclusions can be withdrawn as follows:

- It is rational to calculate RFAC columns' resistance using the proposed nonlinear models of FAC in the forms of bi-linear and tri-linear stress-strain relationships modified from those of OPC concrete with the corresponding modification parameters of ε'_{b1} = 0.0022 and k_E = 0.91 determined from experiment;
- The proposed analytical approach can be sufficiently used for the sectional analysis to provide close and conservative prediction of RFAC columns load resistance. It can also be flexibly modified for any other types of new concrete material provided that an appropriate nonlinear material model is incorporated;
- The experimental program performed at structural level in this study provides new results and observations on the behavior and load resistance of RFAC columns, as well as good validation of the proposed analytical method.

The analytical approach proposed by the authors can be further developed for three-dimensional computational models to apply for RFAC beams, slabs, walls, pipe caps, etc. Besides, studies on Serviceability Limit States of RFAC structures should also be performed in future.

Acknowledgement

The experimental study presented in this article was conducted in Laboratory LAS-XD 125 (HUCE), of which the technicians' efficient support is appreciated by the authors.

References

[1] Bresler, B. "Design criteria of reinforced concrete columns under axial load and biaxial bending", ACI Structural Journal, 57(11), pp. 481–490, 1960. https://doi.org/10.14359/8031

[2] Furlong, R. W., Hsu, C-T. T., Mirza, S. A. "Analysis and Design of Concrete Columns for Biaxial Bending-Overview", ACI Structural Journal, 101(3), pp. 413–423, 2004. https://doi.org/10.14359/13101

[3] Szerszen, M. M., Szwed, A., Nowak, A. S. "Reliability analysis for eccentrically loaded columns", ACI Structural Journal, 102(5), pp. 676–688, 2005. https://doi.org/10.14359/14663

[4] Aschheim, M., Hernández-Montes, H., Gil-Martín, L. M. "Optimal domains for strength of rectangular sections for axial load and moment according to Eurocode 2", Engineering Structures, 29, pp. 1752–1760, 2007. https://doi.org/10.1016/j.engstruct.2006.09.021

[5] Mosley, B., Bungey, J., Hulse, R. "Reinforced concrete design to Eurocode 2", Palgrave MacMillan, 2007. ISBN 978-0-230-30285-3

[6] Wight, J. K., MacGregor, J. G. "Reinforced concrete - Mechanics and design", 6th ed., Pearson Education Inc., 2012. ISBN 0132176521

[7] Tan, K. H., Nguyen, T.-T., Nguyen, T. T. "Discussions on using EN 1992-1-1:2004 in design of precast prestressed planks and biaxially-loaded slender columns", In: Proceedings of the Third International Workshop on Design of Concrete Structures Using Eurocodes, Vienna, Austria, 2012, pp. 203–210. ISBN 978-3-902749-03-1

[8] Tan, K.-H., Nguyen, T.-T. "Experimental behaviour of reinforced concrete columns subjected to biaxial bending and restraint at elevated temperatures", Engineering Structures, 56, pp. 823–836, 2013. https://doi.org/10.1016/j.engstruct.2013.06.013

[9] EN 1992-1-1:2004 "Design of concrete structures - Part 1-1: General rules and rules for buildings", European Standards, 2004.

[10] ACI 318-19 "Building code requirements for structural concrete", American Concrete Institute, Farmington Hills, MI, USA, 2019.

[11] SP 63.13330.2012 "Concrete and reinforced concrete structures - Principal rules", Ministry of Regional Development of the Russian Federation, Moscow, Russia, 2012.

[12] TCVN 5574:2018 "Concrete and reinforced concrete structures - Design standard", Ministry of Science and Technology, Ha Noi, Vietnam, 2018. (in Vietnamese)

[13] ACI 232.2R-18 "Report on the use of fly ash in concrete", American Concrete Institute, Farmington Hills, MI, USA, 2018.

[14] Marthong, C., Agrawal T. P. "Effect of fly ash additive on concrete properties", International Journal of Engineering Research and Applications, 2(4), pp. 1986–1991, 2012.

[15] Mallisa, H., Turuallo, G. "The maximum percentage of fly ash to replace part of original Portland cement (OPC) in producing high strength concrete", AIP Conference Proceedings, 1903, 030012, 2017. https://doi.org/10.1063/1.5011519

[16] Iqbal, S., Ali, A., Holschemacher, K., Ribakov, Y., Bier, T. A. "Effect of Fly Ash on Properties of Self-Compacting High Strength Lightweight Concrete", Periodica Polytechnica Civil Engineering, 61(1), pp. 81–87, 2017. https://doi.org/10.3311/PPci.8171

[17] Kao, Y.-C., Chiu, C.-K., Ueda, T., Juan, Y.-J. "Experimental investigation on mechanical properties of SBR-modified mortar with fly ash for patch repair material", Journal of Advanced Concrete Technology, 16(8), pp. 382–395, 2018. https://doi.org/10.3151/jact.16.382

[18] Kaveh, A., Bakhshpoori, T., Hamze-Ziabari, S. M. "M5' and Mars Based Prediction Models for Properties of Self-Compacting Concrete Containing Fly Ash", Periodica Polytechnica Civil Engineering, 62(2), pp. 281–294, 2018. https://doi.org/10.3311/PPci.10799

[19] Sheen, Y.-N., Le, D.-H., Lam, M. N.-T. "Performance of Self-compacting Concrete with Stainless Steel Slag Versus Fly Ash as Fillers: A Comparative Study", Periodica Polytechnica Civil Engineering, 65(4), pp. 1050–1060, 2021. https://doi.org/10.3311/PPci.17673

[20] Nguyen, T. T. N., Nguyen, A. T., Vu, Q. V., Ngo, V. T., Lam, T. Q. K. "The strength of fly ash of experimental design", Magazine of Civil Engineering", 109(1), 10911, 2022. https://doi.org/10.34910/MCE.109.11

[21] Cross, D., Stephens, J., Vollmer, J. "Structural applications of 100 percent fly ash concrete", In: 2005 World of Coal Ash Conference, Lexington, KY, USA, 2005, pp. 1–19. ISBN 9780967497167

[22] Sumajouw, D. M. J., Hardjito, D., Wallah, S. E., Rangan, B. V. "Fly ash-based geopolymer concrete: study of slender reinforced columns", Journal of Materials Science, 42, pp. 3124–3130, 2007. https://doi.org/10.1007/s10853-006-0523-8

[23] Van den Heede, P., Gruyaert, E., Robeyst, N., De Belie, N. "Life cycle assessment of a column supported isostatic beam in high-volume fly ash concrete (HVFA concrete)", In: RILEM Proceedings, PRO 70, pp. 437–444, 2010. [online] Available at: http://hdl.handle.net/1854/LU-1266046

[24] Muthupriya, P., Subramanian, K., Vishuram, B. G. "Experimental investigation of high performance reinforced concrete column with silica fume and fly ash as admixtures", Asian Journal of Civil Engineering (Building and Housing), 12(5), pp. 597–618, 2011. [online] Available at: https://www.sid.ir/en/journal/ViewPaper.aspx?id=263562

[25] Rahman, M. M., Sarker, P. K. "Geopolymer concrete columns under combined axial load and biaxial bending", presented at Proceedings of the Concrete 2011 Conference, Perth, WA, Australia, Sep, 26–28, 2011. [online] Available at: http://hdl.handle.net/20.500.11937/26268

[26] Albitar, M., Mohamed Ali, M. S., Visintin, P. "Experimental study on fly ash and lead smelter slag-based geopolymer concrete columns", Construction and Building Materials, 141, pp. 104–112, 2017. https://doi.org/10.1016/j.conbuildmat.2017.03.014

[27] Yoo, S.-W., Choi, Y. C., Choi, W. "Compression Behavior of Confined Columns with High-Volume Fly Ash Concrete", Advances in Materials Science and Engineering, 2017, 8208079, 2017. https://doi.org/10.1155/2017/8208079

[28] Othman, Z. S., Mohammad, A. H. "Behaviour of eccentric concrete columns reinforced with carbon fibre-reinforced polymer bars", Advances in Civil Engineering, 2019, 1769212, 2019. https://doi.org/10.1155/2019/1769212

[29] Wang, J. H., Sun, Y. P., Takeuchi, T., Koyama, T. "Seismic behavior of circular fly ash concrete columns reinforced with low-bond high-strength steel rebar", Structures, 27, pp. 133–1357, 2020. https://doi.org/10.1016/j.istruc.2020.07.005

[30] Salla, S. R., Modhera, C. D., Babu, U. R. "An experimental study on various industrial wastes in concrete for sustainable construction", Journal of Advanced Concrete Technology, 19(2), pp. 133–148, 2021. https://doi.org/10.3151/jact.19.133

[31] Dharmaraj, R., Bhadauria, S. S., Mayilsamy, K., Thivya, J., Karthick, A., Baranilingesan, I., Mohanavel, V., Muhibbullah, M., Osman, S. M. "Investigation of reinforced concrete column containing metakaolin and fly ash cementitious materials", Advances in Civil Engineering, 2022, 1147950, 2022. https://doi.org/10.1155/2022/1147950

[32] ASTM C618-12a "Standard specification for coal fly ash and raw or calcined natural pozzolan for use in concrete", ASTM International, West Conshohocken, PA, USA, 2012. https://doi.org/10.1520/C0618-12A

[33] Nguyen, T.-T., Dang. V.-H. "Experimental and Probabilistic Investigations of the Effect of Fly Ash Dosage on Concrete Compressive Strength and Stress-strain Relationship", Periodica Polytechnica Civil Engineering, 66(4), pp. 1098–1113, 2022. https://doi.org/10.3311/PPci.20607